Direct imaging and spectroscopy of habitable planets using JWST and a starshade

Citation: Soummer, Remi et al. "Direct imaging and spectroscopy of habitable planets using JWST and a starshade." Space Telescopes and Instrumentation 2010: Optical, Infrared, and Millimeter Wave. Ed. Jacobus M. Oschmann et al. San Diego, California, USA: SPIE, 2010. 77312I-15. ©2010 SPIE.

As Published: http://dx.doi.org/10.1117/12.858347

Publisher: Society of Photo-optical Instrumentation Engineers

Persistent URL: http://hdl.handle.net/1721.1/61646

Version: Final published version: final published article, as it appeared in a journal, conference proceedings, or other formally published context

Direct imaging and spectroscopy of habitable planets using JWST and a starshade

Rémi Soummer[a], Jeff Valenti[a], Robert A. Brown[a], Sara Seager[b], Jason Tumlinson[a], Webster Cash[c], Ian Jordan[g,a], Marc Postman[a], Matt Mountain[a], Tiffany Glassman[f], Laurent Pueyo[e], Aki Roberge[d]

[a]Space Telescope Science Institute, 3700 San Martin Drive, Baltimore MD 21218, USA
[c]University of Colorado, Boulder, CO 80309, USA
[g]Science Programs, Computer Sciences Corporation
[d]NASA Goddard Space Flight Center, Greenbelt, MD 20771, USA
[f]Northrop Grumman Corporation, Redondo Beach, CA 90278, USA
[b]Massachusetts Institute of Technology, Cambridge, MA 02139, USA
[e]Jet Propulsion Laboratory, Pasadena, CA 91109, USA

ABSTRACT

A starshade with the James Webb Space Telescope (JWST) is the only possible path forward in the next decade to obtain images and spectra of a planet similar to the Earth, to study its habitability, and search for signs of alien life. While JWST was not specifically designed to observe using a starshade, its near-infrared instrumentation is in principle capable of doing so and could achieve major results in the study of terrestrial-mass exoplanets. However, because of technical reasons associated with broadband starlight suppression and filter red-leak, NIRSpec would need a slight modification to one of its target acquisition filters to enable feasible observations of Earth-like planets. This upgrade would 1) retire the high risk associated with the effects of the current filter red leak which are difficult to model given the current state of knowledge on instrument stray light and line spread function at large separation angles, 2) enable access to the oxygen band at 0.76 μm in addition to the 1.26 μm band, 3) enable a smaller starshade by relaxing requirements on bandwidth and suppression 4) reduce detector saturation and associated long recovery times. The new filter would not affect neither NIRSpecs scientific performance nor its operations, but it would dramatically reduce the risk of adding a starshade to JWST in the future and enhance the performance of any starshade that is built. In combination with a starshade, JWST could be the most capable and cost effective of all the exoplanet hunting missions proposed for the next decade, including purpose built observatories for medium-size missions.

Keywords: exoplanets, extrasolar, JWST, occulter, starshade, earth-like, coronagraphy

1. INTRODUCTION

Among the various techniques to discover new extrasolar planets, direct imaging has already produced a few exciting results[1–3] and is poised to expand dramatically with the upcoming commissioning of new ground based instruments on large telescopes.[4–7] These ground-based instruments use high-contrast adaptive optics coronagraphs and spectrographs for detecting and characterizing relatively young giant planets around nearby stars. More ambitious goals such as imaging a terrestrial planet similar to the Earth in the habitable zone of a nearby star requires space based observatories.[8] Imaging can be used for detection, and spectroscopy is required to address the most interesting questions such as habitability and possible presence of life. Several mission concepts are studied for space-based high-contrast imaging missions (see for example http://exep.jpl.nasa.gov/). For visible and near-infrared wavelengths, these missions usually consider internal coronagraphs[9] or external occulters such as New Worlds Observer[10] (NWO) or THEIA.[11] For infrared missions, these missions involve interferometers.[12]

Further author information: (Send correspondence to R.S.)
R.S.: E-mail: soummer@stsci.edu, Telephone: 1 410 338 4737

Space Telescopes and Instrumentation 2010: Optical, Infrared, and Millimeter Wave,
edited by Jacobus M. Oschmann Jr., Mark C. Clampin, Howard A. MacEwen, Proc. of SPIE
Vol. 7731, 77312I · © 2010 SPIE · CCC code: 0277-786X/10/$18 · doi: 10.1117/12.858347

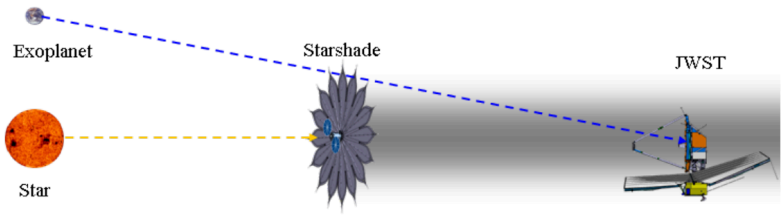

Figure 1. Principle of a starshade on a separate spacecraft to block the light from the star, while allowing the light from an exoplanet to pass the edge of the occulter unimpeded. Figure credit: Northrop Grumman Corporation.

The basic principle of the starshade is shown in Figure 1, where the occulter is used to cast a shadow from the star onto the telescope, therefore canceling the direct star light while the light from a planet is not affected. With two spacecraft involved (the telescope and the starshade), occulter missions are typically in the flagship cost range, well above one billion dollars. However, both the THEIA and NWO studies have shown that most of the cost resides in the telescope. An occulter mission can be envisioned for a medium mission cost if it uses an existing or already planned host telescope can be found, or a small ($\simeq 1.2m$) off-the-shelf telescope.[13] In this white paper, we discuss using the James Webb Space Telescope[14,15] for this purpose[16,17] using a 65 m starshade (tip to tip) at 67,000 km distance from the telescope, with a geometric inner working angle of 0.1 arcsec. The distinct mission concept of a starshade for JWST has been adapted from the NWO concept and is called the New Worlds Probe to distinguish it from its larger telescope + occulter cousin.[16,17] With JWSTs large aperture and high sensitivity,[14] a starshade would enable images and spectra of extrasolar planets with sufficient contrast and inner working angle (the smallest angular separation at which a planet can be distinguished from the parent star) to discover planets down to the size of the Earth in the habitable zone around nearby stars. Such a combination would address a series of fundamental questions: are there habitable planets? What is the composition of their atmospheres? What are the properties of exozodiacal disks around nearby stars? What is the mass and composition of currently known giant planets? Because large apertures in space are required to address these questions,[8] a starshade with JWST is a particularly interesting opportunity for the coming decade and would serve as a precursor for much more ambitious projects such as ATLAST[18,19] and would solve unknowns about the exozodiacal brightness and structure, which is critical for future flagship missions.[20]

Our Design Reference Mission shows that five habitable Earth-mass planets could be detected and characterized, assuming an occurrence rate for these planets of 30%. This would be a valuable addition to JWSTs science program. The science goals for NWP are very competitive compared to a small (1-1.5m) coronagraphic telescope as discussed in the Exoplanet Community Report,[21] mainly in terms of spectroscopic characterization capabilities, which are not possible with small telescope. The objectives are articulated around three main themes:[22] 1) Identifying habitable terrestrial planet and searching for indications of life. 2) Characterization of known planets from radial velocity surveys. 3) Measuring and Characterizing Exozodiacal disks around nearby stars.

Designing a starshade addition for JWST includes a number of challenges because the observatory was not designed for this particular application. In this paper, we focus on the discussion of the science capabilities given existing instruments, and study the science program and starshade design optimization given the constraints of NIRCam (Near-Infrared Imaging Camera), and NIRSpec (Near Infrared Spectrograph).

In principle, it is possible to find a starshade solution (i.e. a combination of starshade diameter, distance, and petals shape) for any spectral bandwidth. However, the starshade is mostly constrained by the longest wavelength of the band because of the physics of Fresnel diffraction by the starshade occulter. The larger the bandpass, the larger the starshade. Outside of the optimal bandpass, the starshade starts to leak starlight, and the leakage is more serious on the red side of the band. In Figure 2, we show a possible starshade starlight suppression profile, where the starshade suppresses the light at the 10^{10} level up to 2.0 μm. At 5.0 μm, the starshade suppression is less than 100. JWST detectors are sensitive to a large range of wavelengths. The short wavelength arm of NIRCam is sensitive from 0.6 to 2.6 μm, and the NIRSpec detector is sensitive to the full range from 0.6 to 5.0 μm. Because of the range of sensitivity of the NIRCam and NIRSpec detectors, filters would be required to compensate for the starshade red leak and to block the light outside of the optimal starshade region up to the limit of sensitivity of the detector. In the case of NIRCam imaging, any leakage through the

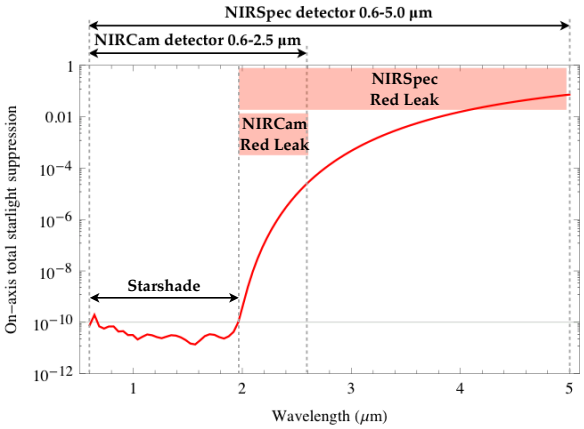

Figure 2. Illustration of the red-leak problem associated with the design of a starshade for JWST. The red line shows a possible starshade starlight suppression profile. The range of sensitivity for the NIRCam and NIRSpec detectors are indicated by the black arrows. The red rectangles show the wavelength regions where the starlight suppression must rely on filters out-of-band rejection. with NIRSpec, a target acquisition filter can be used with the starshade to reduce the red leak. The range of wavelengths is larger for NIRSpec but the effect of the red leak is alleviated by the dispersion. In first approximation, the residual starlight is the product of the starshade suppression profile by the filter transmission.

imaging filters is very damaging to the performance because the star image would be extremely bright at longer wavelengths. In the case of a spectrum, the red leak effects are mitigated by the dispersion because the longer wavelength light does not hit the same location as the planet on the detector, except for the effects caused by the line spread function and the stray light. In Section 2, we consider the constraints on the starshade design imposed by the actual NIRCam filters transmission. For NIRSpec, a target acquisition filter could be used as a blocking filter to alleviate this issue. However, the current target acquisition filter (F140X), with a bandpass from 0.8 to 2.0 μm has a significant red leak around 2.5-3μm. In section 3 we assume for the calculations that this filter is upgraded with a better quality filter with 10^5 out-of-band rejection, and slightly revised bandpass to optimize the science program.

2. IMAGING PERFORMANCE AND GOALS

2.1 Scientific goals

Using NIRCam imaging, broadband images of planets and disks are achievable in very reasonable exposure times, a true Earth-twin in about 20 hours, and a 5 Earth-mass Super-Earth in the habitable zone of a Sun-like star at 10 pc in about two hours. Although JWSTs aperture is segmented with modest optical quality (diffraction limited at 2 μm), the starshade prevents the light from entering the telescope and NWP is almost insensitive to JWSTs optical quality at short wavelengths.The available NIRcam filters can also provide preliminary color information that can be used to decide spectroscopic followup with NIRSpec. In particular, two medium band filters (F140M and F162M) can be used to detect water in the atmosphere.

Although mass is not directly measurable by imaging alone, colors and low resolution spectroscopy can provide some preliminary diagnostic of the terrestrial nature and habitability of the planet. For a terrestrial planet, the habitability is defined from the presence of water vapor in its atmosphere, which suggest the presence of liquid bodies of water at the surface. The near infrared is particularly suited for the detection of water, which is readily detected with a low resolution (R$\simeq$40) available with the NIRSpec prism. In Figure 3, we show a model spectrum of the Earth atmosphere, and with the actual NIRCam filters transmission applied to the spectrum.

These broadband and medium band filters can be used for color information. Figure 4 shows a color-color diagram for the four atmospheric models of terrestrial planets used in this white paper. The vertical axis gives an indication of the presence of water using the two medium band filters. This distinguishes for example the Earth atmosphere from the Venus-like atmosphere with only CO_2. The horizontal axis provides an indication for the presence of CH_4 or CO_2, which affects mostly the F150W measurement. Other combinations of colors

can be studied with the set of available filters. This type of color information if limited and should be used with caution, but can be used after NIRCam imaging to guide the decision of a spectroscopic followup.

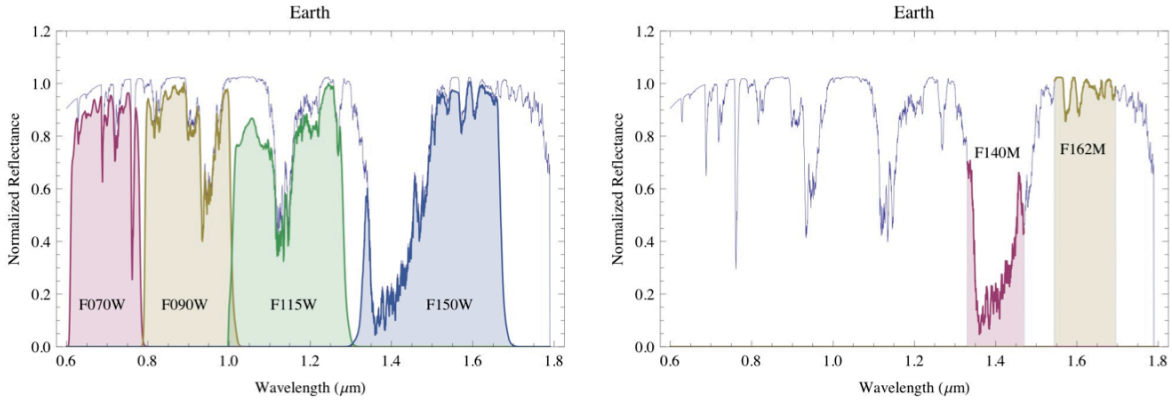

Figure 3. NIRCam broadband filters super-imposed with Earth model spectrum. In addition to the broadband filters, two medium band filters are particularly interesting to to study the presence of water bands.

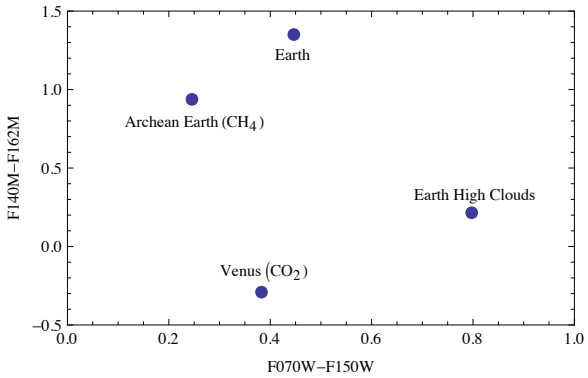

Figure 4. Color-color diagram for the four model atmospheres of terrestrial planets used in this paper, using a set of NIRCam filters. The vertical axis corresponds to the on/off water band filters. The horizontal axis is influenced by long-wavelength methane or carbon dioxide absorption. This type of diagram can be used to evaluate which targets are most interesting for spectroscopic followups with NIRSpec.

2.2 Exposure Time Calculations

Several elements are included in the exposure time calculation for NIRCam. The calculations are made for an Earth atmosphere, and we assume an albedo of 0.26 to be consistent with other studies for terrestrial planet searches.[23,24] Since we are interested in the detectability in the near infrared, we calculate the albedo for each of the NIRCam filters using an Earth spectrum, assuming an albedo of 0.26 in the V band. We find the albedos for each filter to be: F070W:0.24, F115W: 0.19, F150W: 0.1, F140M: 0.02, F162M: 0.18. Because of the water bands the albedo can be significantly lower in some filters. Note the case of filter F140M, where the Earth albedo is virtually zero, because it is located at a deep water band absorption. The star is assumed to be the Sun at 10 pc. We follow the signal to noise ratio (S/N) calculation described by Brown,[23] using the parameters provided by the NIRCam team (private communication). We add the exozodiacal contribution to the background. For an exozodiacal disk identical to the solar system zodiacal disk, the total background surface brightness is three zodis, where one zodi is the surface brightness of the local zodiacal light. We add a 20% margin to the total background to be consistent with the general approach used with NIRCam. The S/N calculation also includes the residual starlight counts, and we assume that the surface brightness of starlight is suppressed to a contrast of 10^{-10} in the search region, which accounts for starshade imperfections (the perfect starshade design delivers a significantly higher contrast at the search location). The S/N calculation does not need any additional red

leak contribution since for NIRCam, the overall suppression is 10^{-10} over the entire range of sensitivity of the detector (starshade, QE, dichroic, and SED). We cross checked our S/N calculation with the estimations for NIRCam and our estimations are consistent without starshade.

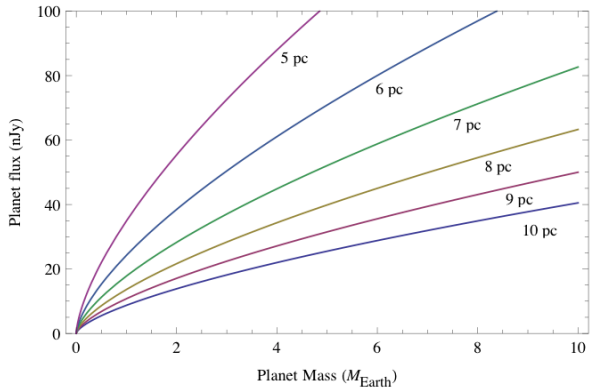

Figure 5. Planet flux for a terrestrial planet around the Sun as a function of distance and planet mass. The planet is at 1 AU at quadrature, and assumed to have the same density and albedo as the Earth. The Earth at 10 pc which we use throughout this white paper is a very difficult target, but the situation is dramatically relaxed with more massive planet and/or closer stars. There are respectively (17,33,46,56,74,95) stars in the TPF catalog in this range of distances (5-10 pc). More stars might be observable with a more inclusive catalog. Since observations are background limited in most cases of interest exposure time scales with the square of the planet brightness.

In the background limited regime, which is the case for a typical Sun at 10 pc, the strong dependence of the exposure time with the planet brightness favors super-Earths. Indeed, assuming same albedo and density as the Earth, a 5 Earth mass planet is about 3 times brighter than an Earth twin and therefore the exposure time is eased by almost an order of magnitude (Figure 5). This is illustrated in Figure 6 and 7 where we give the details of the exposure time calculation result for each NIRCam filter of interest for an Earth twin, and a 5 Earth mass planet, both with a 1AU separation around the Sun at 10 pc. Exposure times well under an hour can be obtained with slightly more favorable objects, e.g. closer to the inner edge of the habitable zone, more massive, or with higher cloud coverage and/or higher albedos. For examples with Venus albedo, these exposure times would be typically 6 times shorter and the planet would be detectable in minutes for a 5 Earth mass planet. These calculations are based on the requirement equivalent read noise for a 1000s for the entire chip, which is conservative because starshade observations would use subarray modes with significantly reduced read noise.

Filter Name	wavelength (μm)	Star (Jy)	Contrast	Δm	ExpTime (s)	ExpTime (hours)
F070W	0.7	54.1	3.87×10^{-10}	23.53	18,522	5.1
F115W	1.15	58.2	3.17×10^{-10}	23.74	8,257	2.3
F150W	1.5	52.4	1.73×10^{-10}	24.4	30,525	8.5
F140M	1.4	53.7	3.52×10^{-11}	26.13	2,180,470	606
F162M	1.62	50.6	3.03×10^{-10}	23.8	33,742	9.4

Figure 6. Same as previously in the case of a 5 Earth mass planet, assuming same density, albedo and atmospheric features. The exposure times are a few hours for most filters, and can be made well below an hour with a slightly more favorable planet e.g. high clouds, more massive planet, closer distance. For example, a planet with Venus albedo would require exposure times typically 6 times shorter and would be detectable in minutes.

3. SPECTROSCOPIC PERFORMANCE AND GOALS

3.1 Scientific goals

Direct images of exoplanets can have a tremendous impact on the community and on the public, but are not sufficient to address the most interesting science goals. The highest priority for a future possible starshade with JWST is to ensure spectroscopic capabilities. A number of biomarkers can be studied in the bandpass and

Filter Name	wavelength (μm)	Star (Jy)	Contrast	Δm	ExpTime (s)	ExpTime (hours)
F070W	0.7	54.1	1.32×10^{-10}	24.70	155,627	43
F115W	1.15	58.2	1.08×10^{-10}	24.91	69,018	19
F150W	1.5	52.4	5.91×10^{-11}	25.57	258,077	72
F140M	1.4	53.7	1.20×10^{-11}	27.30	18,606,700	5169
F162M	1.62	50.6	1.04×10^{-10}	24.96	284,017	79

Figure 7. Exposure time calculations for each of the NIRCam filters assuming an Earth twin around the Sun at 10 pc. The calculation includes an exozodiacal disk identical to our solar system disk with a 20% margin applied to the total background. The brightness of the planet accounts for the spectral features included in the effective albedo for each filter. All these estimations are background limited. Note that F140M corresponds exactly to a water band and a non-detection in this filter together with a detection in F162M would be most interesting.

spectral resolution accessible to JWST. Figure 8 shows the NIRSpec extracted counts for three types of model atmospheres of terrestrial planets, using the low-resolution prism. The first spectrum is current day Earth model including oxygen, ozone, water, carbon dioxide. The second model is an Archean Earth rich in methane with 1000x the current abundance, and without oxygen or ozone. The third model is a Venus-like atmosphere entirely dominated by carbon dioxide.

In this section we describe the expected performance with an upgraded target acquisition filter. NIRSpec can address the habitability of a terrestrial planets by detecting water vapor in its atmosphere using the low spectral resolution prism (R$\simeq$40) at short wavelengths ($< 1.5\mu$m). For a 5 Earth-mass planet, a 5σ detection of the water feature is achieved in only about 2.5 hours, and in about 20 hours for a true Earth-twin at 10 pc. For a Super-Earth, it might even be possible to detect both oxygen lines at 0.76 μm and 1.26 μm, and therefore address the question of life on the planet. The 1.26 μm band is weaker than the 0.76 μm band, but NIRSpec has a much higher sensitivity than at short wavelengths. This measurement would be particularly challenging and would require long exposure times but would potentially lead to the discovery of life on another planet. Figure 9 shows a NIRSpec simulation of 5 Earth-mass planet in the habitable zone of a sun-like star at 10 pc, with appropriate resolution to detect the oxygen band. Assuming appropriate zodiacal background, and very pessimistic line spread function and stray light contamination (but not the contamination from other grating orders), we find that both oxygen bands at 0.76 μm and 1.26 μm can be detected in respectively 1.2×10^6 s, and 10^6 s with 3σ significance for a 5 Earth mass planet at 1AU.

The low-resolution mode with the prism has sufficient resolution to identify the main possible molecules in the atmosphere of a terrestrial planet (H_2O, CO_2, CH_4) and to differentiate types of planet provided sufficient signal to noise ratio, which should be obtainable with exposures comparable to that required for the detection of water (typically a few tens of hours for an Earth twin). For example, the range of wavelengths chosen for the upgraded filter would enable to differentiate the current Earth from an Archean Earth rich in methane or from a Venus-type atmosphere rich in carbon dioxide (Figure 8).

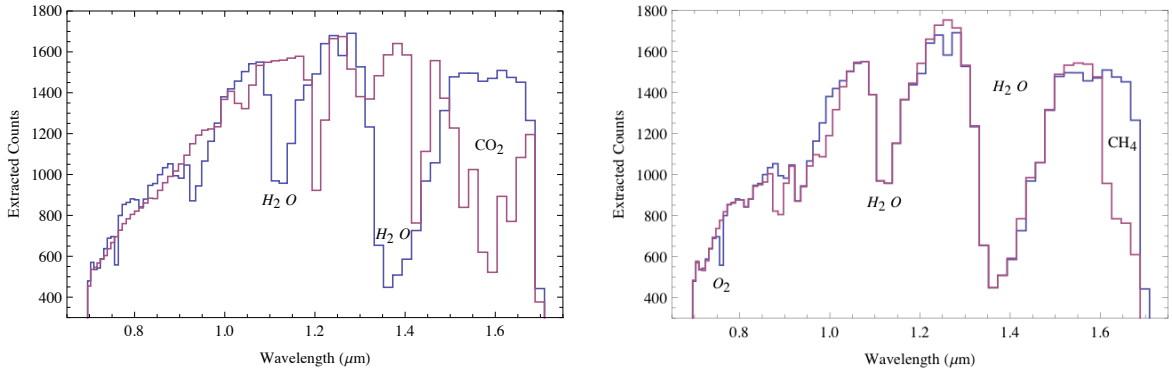

Figure 8. Comparison between a current Earth (blue) and an Archean-Earth (red) rich in methane (CH4) and without oxygen (O2). Water is detected in 20 hours at the 5σ level. Comparison between a current Earth (blue) and a Venus-type atmosphere (red) rich in carbon dioxide (CO2), which has several features especially between 1.4 and 1.7 μm.

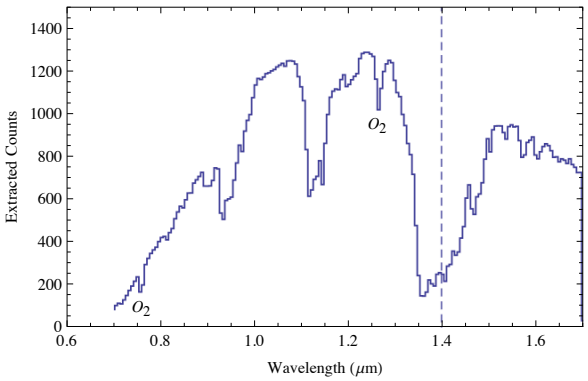

Figure 9. Simulation of a super-Earth spectrum (5 Earth mass) using the R=1000 grating and rebinning the spectrum down to R 100. The simulation assumes the use of a new filter F170S from 0.7 to 1.7 μm, which places the second-order contamination beyond 1.4 μm (dashed line). The calculation assumes a diffraction limited Line Spread Function for the spectrograph (without contribution from the zeroth or higher orders). The prism can be used to detect the 0.76 μm band. This figure does not include noise, but included in the calculation of the significance of the detection.

3.2 Exposure Time Calculations

We follow the method used for the estimation of the NIRSpec S/N and exposure time (Jakobsen, private communication). We add the residual starlight,[23] and additional background for the exozodi. We assume that the surface brightness of starlight is suppressed to a contrast of 10^{-10} in the search region, as in the NIRCam case (this accounts for starshade imperfections). To cross check our S/N calculation with estimates for NIRSpec, we verified the sensitivity limit for the detection of the continuum in the case of total starlight extinction.

We also use a separate code by Valenti to produce simulated spectra. Here, we revisit the choice of parameters for the starshade simulation. We calculate the sampling up the ramp (aka multiaccum) assuming a double correlated sampling noise per pixel of σ_{CDS}=25 e-/pixel (rms). For full-frame read-outs, with 23 groups of 4 averaged frames, this corresponds to the NIRSpec total noise requirement of σ=6 e-/pixel (rms) for a 1000 s integration, with a 10.6 s frame read time. The spectra in starshade mode would be acquired with a 0.2×3.5 arcsec slit, and we would use the 64×2048 subarray mode, for which each frame read time is 1.325 s. We consider 1000s integrations (one ramp) each consisting of 190 groups of 4 averaged frames. All simulated spectra in this paper showing collected counts correspond to a 10^5s exposure (100 integrations). The noise performance of sub-array mode has not been fully tested yet, so it is currently unclear whether the variance will continue to scale with the number of groups per 1000s integration, which is a factor of 8 larger in subarray mode. Here we assume the optimistic case and we use read noise rms value of σ=2.2 e-/pixel for a 1000s integration. The way the spectrum is extracted and the way the background is estimated from the data has important consequences in the S/N estimation and we detail below the assumptions we use in our calculation. A higher S/N is achieved if the signal can be extracted from a smaller number of pixels (noise pixels). In our calculation, we use a number of signal pixels npix=6 (i.e. 3 spatial pixels by 2 spectral pixels per resolution element). Pixels are 0.11 arcsec in the spatial direction. npix=8 would be a more conservative case appropriate for marginally extended faint galaxies. Several backgrounds need to be carefully considered. Contaminations to the planet spectrum include residual starlight (starshade leak), exozodiacal disk, which is expected to be spatially limited, and local zodiacal background, stray light and detector bias. The 64×2048 pixels sub-array mode corresponds to 6 arcsec in the spatial direction, which is significantly larger than the slit (3.5 arcsec). We assume that detector bias, stray light and local zodiacal background can be estimated from a large number of pixels, beyond the extension of the exozodiacal disk ($<$ 1 arcsec) or beyond the extension of the slit. Therefore, we assume that the uncertainty on the mean for the detector biases, local zodi and stray light has a negligible influence on the final S/N. The key parameter corresponds to the ratio of target pixels to the number of pixels used to estimate the background. For the exozodiacal light the number of spatial pixels is small because the detectable exozodi size is a few AU. However, we consider that all the spectral pixels can be used simultaneously to estimate the exozodi background assuming that the zodi spectrum is similar to the star to a scattering function. In other words, we assume that negligible variance is added to the S/N calculation when subtracting the background because the background

can be estimated from a much larger number of pixel than the target.

Other parameters that may depend on specific assumptions include OTE efficiency ($\simeq$0.8), slit efficiency ($\simeq$0.7), optics efficiency ($\simeq$0.6), and QE ($\simeq$0.8). In all NIRSpec calculations we assume a conservative stray light level of one zodi, and therefore use a total of 4 zodis for the background, where one zodi corresponds to a surface brightness of 0.15 MJy/Sr. We also apply a 20% margin to the zodiacal background, following the usual practice for JWST. With all these assumptions observations are also background limited in the case of the low resolution prism for an Earth twin at 10 pc. Because of the background limited regime, the exposure times are also much shorter for larger planets.

There are potentially two oxygen bands accessible to NIRSpec with the proposed filter F170S (0.7-1.7 μm). We use a simulation of the spectrum to study the detectability of both features. The 1.26 μm feature is weaker than the 0.76 μm A band, but compensated by a much higher NIRSpec sensitivity (Figure 9). The R=1000 grating is required for the study of the 1.26 μm, but the prism gives a better sensitivity for the 0.76 μm band, which is mostly explained by the poor efficiency of the grating at short wavelengths (blaze angle at 1.4 μm). Overall the 1.26 μm band provides a slightly better detection. The possibility of detecting both oxygen bands is a unique capability of JWST+starshade and add confidence to a detection.

We use this simulation to address the detectability of oxygen. The simulation uses the R=1000 grating and collected pixels are binned down to a resolution of R=200 at the O2 band (1.26 μm). We select 4 bins to define the line, and 5 bins on the left and 3 bins on the right of the line to define the continuum, as shown in Figure 9.

We estimate the observable line depth $D = 1 - L/C$ for the total signal, where L corresponds to the mean counts for the line bins, and C corresponds to the mean continuum counts. The continuum at the location of the line is estimated to be 1259 +/- 88 detected photons per bin, where the mean of the continuum is estimated by fitting a slope to the selected continuum bins. The variance of the continuum is then estimated from the total collected counts at these bins. Similarly, the line level is estimated to be 1224+/-124 detected photons per bin. The mean line depth of this line is therefore 0.104. The variance of the line depth is obtained an error propagation method as follows:

$$\sigma_D^2 = \left(\frac{\partial D}{\partial C}\right)^2 \sigma_C^2 + \left(\frac{\partial D}{\partial L}\right)^2 \sigma_L^2, \tag{1}$$

$$\sigma_D^2 = \frac{L^2}{C^2}((\frac{\sigma_c}{c})^2 + (\frac{\sigma_L}{L})^2). \tag{2}$$

We obtain a depth of 0.107 +/- 0.116 detected photons per bin, corresponding to a 0.92σ detection of the oxygen band in 10^5 s. We can then scale the exposure time for a 3σ detection, and we find that an exposure time of 1.06×10^6 s is required to detect the oxygen band at 1.26 μm in the atmosphere of a 5 Earth mass planet at 1AU of the Sun at 10 pc. If we assume that the depth does not depend on planet mass, the detection of oxygen would be facilitated for larger planet masses (figure 10). However, the line strength depends on the scale height H$\sim$kT/mg, and the gravity increases with mass as g $\sim$M$^{1/3}$ assuming constant density, so larger mass means weaker signal. The line width is expected to increase with pressure broadening for a larger planet. It is not directly obvious how the detectability is affected by mass, and a detailed calculation is needed. DesMarais[25] gives a curve of growth for the 1.26 μm band with a depth of 0.153 for Earths abundance (21%), and up to 0.23 for 50% abundance. The difference with our measured depth (0.104) can be explained by our estimation from a few binned pixels based on a simulated spectrum which might have slightly different conditions, and because we measure the depth in the presence of background light. An interesting calculation would be to evaluate the detectable abundance for a given planet mass.

We use the same method to calculate the detectability of the oxygen A band. In this case the grating efficiency would prevent the detection in reasonable exposure times (3×10^6s for a 3σ detection). The prism has a low resolution at this wavelength, but would still enable the oxygen detection at the 3σ level in 1.2×10^6 s for a 5 Earth-mass planets at 10 pc. The most optimistic assumptions in our simulations are that the backgrounds can be estimated without any additional penalty, especially for the exozodiacal background for which this requires the use of spatial and spectral pixels simultaneously. The other optimistic assumption is the averaging of the read

noise for subarray modes. The assumptions in terms of line-spread function and stray light are very pessimistic, as detailed below, but assume that the stray light background is relatively uniform and can be calibrated and subtracted.

Planet type, Mass	Separation (AU)	distance (pc)	significance	ExpTime(s)	ExpTime (hours)
Earth-like, 5 M_{Earth}	1	10	3 σ	1.06×10^6	295
Earth-like, 5 M_{Earth}	0.8	8	3 σ	436,000	121
Earth-like, 8 M_{Earth}	1	10	3 σ	574,000	160
Earth-like 8 M_{Earth}	0.8	8	3 σ	236,000	66

Figure 10. Exposure time estimation for the detection of 1.26 μm oxygen in the atmosphere of a habitable terrestrial planet. The exposure time is calculated for a 3σ detection of the spectral feature, based on an estimation of the measurement of the line depth. The simulation includes residual starlight, and background, but does not include contamination from zeroth order, and higher order diffraction. The calculation include a stray light within NIRSpec of 5% of the total red leak counts, and LSF wings 100 x worse than the diffraction limited profile. .

We study the detectability of water using the method, and give exposure time estimations (5σ) in Figure 11 for the detection of the water bands in the $0.7 - 1.7\mu$m bandpass . The detection of water if facilitated by the existence of three large bands between 0.7 and 1.7μm.

Planet type, Mass	Separation (AU)	distance (pc)	significance	ExpTime(s)	ExpTime (hours)
Earth-like, 1 M_{Earth}	1	10	5 σ	73,400	20
Earth-like, 5 M_{Earth}	1	10	5 σ	8600	2.4
Earth-like 5 M_{Earth}	0.8	8	5 σ	3600	1

Figure 11. Exposure times required for a 5σ significance detection of water with the prism, assuming zodiacal and exozodiacal background, one additional zodi for telescope stray light, LSF wings 100x worse than the diffraction limit and stray light contamination of 5% of the total red leak light within NIRSpec. .

4. CONSTRAINTS ON STARSHADE DESIGN FOR JWST

The actual transmission of the NIRCam filters is not perfect with an out-of-band transmission in the range 10^{-4} to 10^{-6}. For the evaluation of the red leak impact on the detection capabilities at shorter wavelengths, the important parameter is the number of star counts collected from the longer wavelengths. Using the Sun spectral energy distribution (SED) as a template, the decreasing counts in the near infrared helps the red leak problem by a factor of several. We calculate for each filter the maximum red leak including actual filter transmission, QE, dichroic and star SED (assuming the sun), and deduce the required starshade suppression at the same wavelength (Figure 12). The criterion is simply that the overall suppression including starshade and other effects must be ten orders of magnitude. This guarantees that the error budget is largely dominated by the background light and not affected by the red leak contribution through the filters. F090W is the worst filter and would require a starshade suppression of 1.44×10^{-7} at 2.57 μm. In the current state of the starshade design possibilities, this would drive the optimization of starshade to an unreasonable size. Discarding F090W for the moment, the red leak requirement is set by the filter with the longest wavelength red leak (F150W) and the starshade suppression requirement is set to 8×10^{-6} at 2.27 μm. This requirements accommodates the red leaks of the three broadband filters F070W, F115W, and F150W. In addition to these broadband filters, two medium band filters are of great interest (F140M and 162M) for the detection of water but the effect of their out-of-band transmission remains to be studied, and they may place new constraints on the starshade design.

In principle either of NIRSpecs two target acquisition filters could be used with the starshade as blocking filters to alleviate the starshade's inefficiency at long wavelengths. The most interesting one for the starshade science goals is the Broadband B filter (F140X). The bandpass goes from 0.8 to 2.0 μm. The filter has a red bump around 2.6 μm of several percent, and a significant transmission almost all the way to the NIRSpec detector cutoff at 5 μm. This is not a problem at all for regular target acquisition activities, but would create significant leak when combined with the starshade (the product of the filter transmission by the starshade suppression profile). Because of this red leak and its associated speckle noise, spectroscopy with NIRSpec and a starshade may not be possible at all with the current filter. This would impact all the science cases presented in this study.

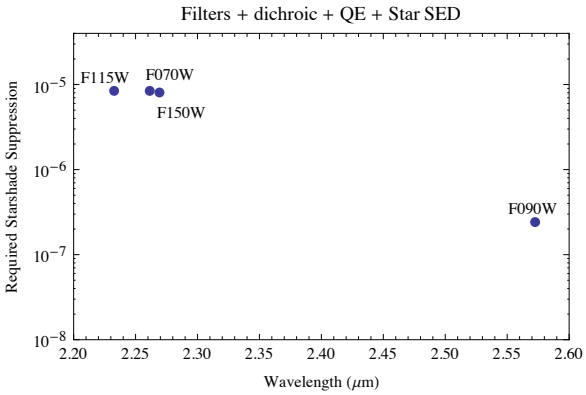

Figure 12. Required starshade suppression as a function of wavelength for the four NIRcam broadband filters. The suppression is defined at the worst out-of-band transmission for each filter so that the overall suppression including all effects is ten orders of magnitude.

The two main parameters for the filter are the bandpass and the out-of-band transmission. Since the Broadband B filter bandpass is loosely defined to enable faint target acquisition, it may be possible to modify the bandpass slightly from 0.8-2.0 μm to 0.7-1.7 μm. If the new filter (here named 170S) has the same in-band transmission as the current one, target acquisition exposures will be about 20% longer. This effect will not be noticed because target acquisition is overhead dominated. On the long wavelength side, starshade optimization is facilitated by a narrower bandpass. However, the red leak of NIRCams filters at 2.27 μm impose a constraint on the minimum starshade size, so there would not be any advantage for the starshade in reducing the NIRSpec bandpass further. Moreover, including 1.7 μm in the transmission band of the new filter covers several bands of water, CO_2, and CH_4 (see Figure 8), and it provides a nice overlap with the NIRCam filter F150W and other filters at shorter wavelengths for cross-calibrations. There is a clear motivation to extend the short cutoff of the new filter as far as possible to include the oxygen A band at 0.76 μm; the short wavelengths do not further constrain the starshade diameter. However, the detection of the oxygen band is challenging due to the low sensitivity of NIRSpec at short wavelengths (the R=1000 grating is blazed at 1.4 μm), and it turns out that the prism has a better sensitivity for the 0.76 μm band despite its lower resolution. A short cutoff of 0.7 μm for the new filter would also cover the 1.26 μm oxygen band with the R=1000 grating without perturbation by the second-order spectrum from below 0.6 μm. The required filter would need an out-of-band transmission of 10^{-5} based on our estimations including NIRSpecs stray light and line spread function estimations. This out-of-band rejection is comparable with the performance of currently-built NIRCam filters.

We show the extracted counts for a 10^5s exposure for an Earth-twin in Figure 13. The new filter reduces the starlight counts by a factor of 10 beyond 4 μm, and by up to 3 orders of magnitude between 2 and 4 μm. In the absence of stray light, and assuming an unrealistic diffraction-limited line spread function the in-band red leak contamination is less than 10 extracted counts per pixel with the new filter. With F140X, the counts are about 100 times higher ($\simeq$1000 counts per pixel). This difference will be amplified when considering realistic levels for the actual line spread function and for the stray light. Assuming a 10$\times$ increase of the far wings of the line spread function, and a very pessimistic stray light level of 5% of the total red leak contaminating the 64×2048 subarray, there is hardly any red leak contamination with the proposed filter, but a very significant background with the current filter (Figure 14). In these figures, the zodiacal background was subtracted to visualize the contribution of the red leak contamination. Note that if this red leak background could be subtracted properly, the additional photon noise would not be a problem because the S/N is vastly dominated by the zodiacal noise. The real problem stems from the fact that the red leak component is formed of speckles, and that their incomplete subtraction will leave residual speckle background, which cannot be modeled at this stage of the study.

5. DESIGN REFERENCE MISSION RESULTS

The purpose of a design reference mission (DRM) is to measure and illustrate scientific performance of a particular mission concept, in this case the power of JWST operating with a starshade to discover Earth-like extrasolar

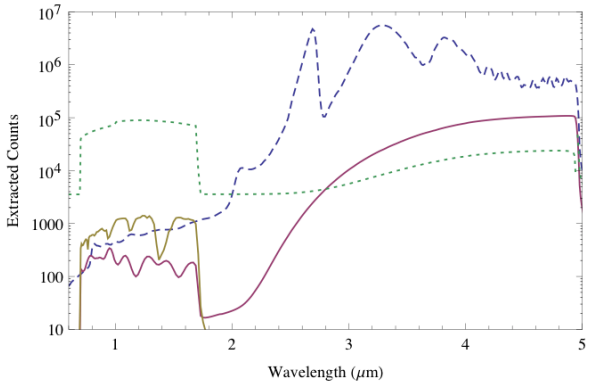

Figure 13. Starlight counts with the starshade and using F140X (dashed blue line), and the proposed filter F170S (red). This new filter alleviates the red leak by two to three orders of magnitudes. Planet counts alone are shown in yellow, and backgrounds in green. In this figure stray light and contamination other diffraction orders are not included, and an optimistic diffraction-limited line spread function is used. Most of the contamination from the red-leak light (3-5 μm region) will occur from stray light and from the far wings of the line spread function.

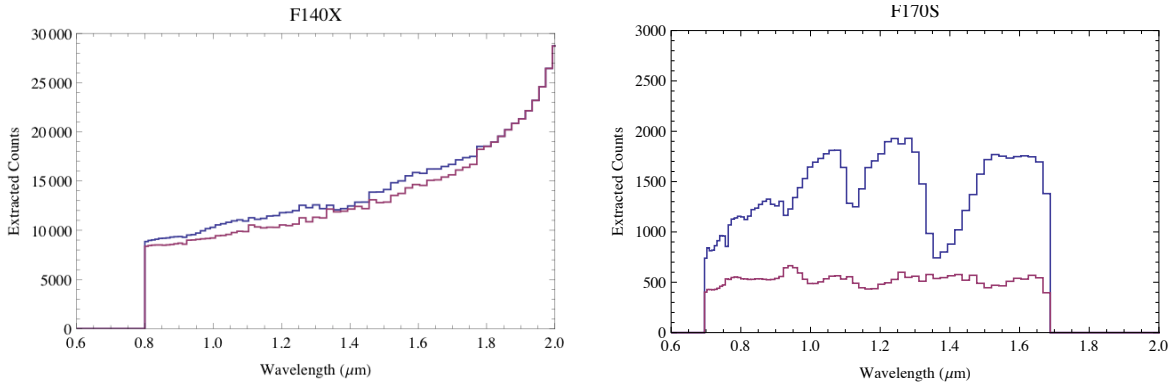

Figure 14. Left: Comparison between the extracted counts for star+planet (blue) and with the red leak contribution using F140X, assuming 10x worse LSF wings and 5% total stray light contaminating the subarray on the detector. Other backgrounds have been subtracted. Note that even in this case, there would be no significant impact if the red leak component could be subtracted without penalty. However, this red leak component will be formed of speckles (not simulated here) and it is uncertain what fraction of theses speckles could be calibrated and subtracted. Right: same simulation, but with a new filter F170S. Here the out-of-band rejection is assumed to be 10^5. In this case, the contamination from the red leak is rendered negligible by the filter transmission. There is no additional speckle background to consider in the calculation of the S/N.

planets. The basis of a DRM includes a science strategy, an input catalog of stars, a definition of the planets of interest (POIs), an estimate or assumption of their occurrence rate η, the performance parameters of the telescope, starshade and instruments, and finally, any constraints, restrictions, and priorities for the planning and scheduling of observations. The report of a DRM includes a statistical representation of science to be expected, plus insights into the character of the mission, from a science-operational point of view. In the current case, our DRMs provide estimates of the number of Earth-like planet discovered and characterized (m), as a function of η (their expected occurrence rate), and the cumulative observing time (here we assume a total observing time of 10^7s). The DRM also verifies our concept of integrating starshade observations into JWST science operations with realistic times allowed for data transfer and the authorization, planning, and scheduling. The most important result of a mission simulation is the probability distribution function for the number of the number of discoveries.[26] Assuming 10^7s for this entire DRM (7-9% of JWSTs observing time), we find that the mean discovery is 5.5 habitable Earths (standard deviation 1.2) discovered and characterized with NIRCam images with 5 filters, and one low-resolution spectrum obtained with NIRSpec. This result assumes an occurrence of Earth-like planets η=0.3. This result would be significantly improved for higher mass planets (e.g. 5 Earth-mass).

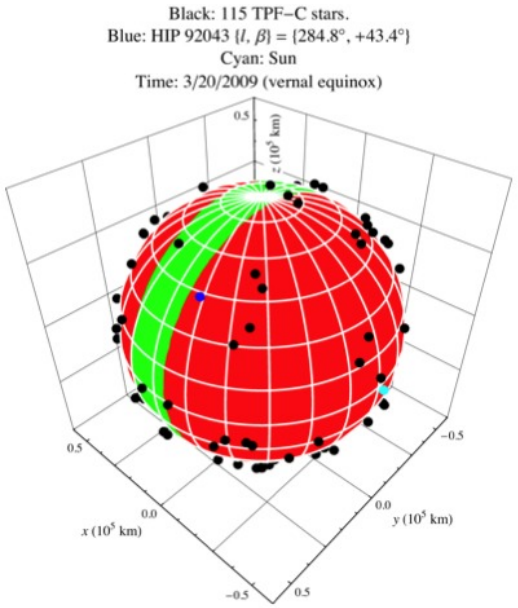

Figure 15. The sphere of starshade operations on the vernal equinox, showing permitted pointings (green), forbidden pointings (red), a typical target star with coordinates provided (blue), the other 115 TPF-C stars (black), and the Sun (cyan), which is fixed in this L2 coordinate system. As time passes, the target stars revolve on the starshade sphere in the clockwise direction as seen from above.

DRM results depend on the particular strategy chosen for the mission. The science strategy of our DRMs is, first, to conduct limiting search observation (LSOs) of nearby stars and second, to immediately characterize any planets discovered with follow-on observations. That is, each LSO is planned with sufficient time available to perform all the desired observations in a single observability window. This mitigates the risk of losing a planet before it can be characterized, with no estimate of the orbit and therefore no means of predicting its recovery. An LSO is an image obtained by NIRCam with sufficient exposure time to achieve S/N = 5 on a source of $\Delta mag_0 = 26$ located outside the inner working angle IWA = 0.085 arcsec around the target star. Δmag_0 is the maximum magnitude difference between the star and the planet that is achievable due to speckle instability (Brown 2005). For each star, we choose the preferred NIRCam filter for the LSO to be the one offering the highest discovery rate. The discovery rate is the probability of a discovery divided by the observing time for the LSO, which is the exposure time plus a fine-alignment time of 10 hours for the starshade. Possible filters with NIRcam are F070W, F115W, F140M, F150W, or F162M. The followup characterization observations have exposure times calculated to the depth of the source actually discovered. Rather than conduct Monte

Carlo experiments at this branch point in simulation, we chose to expose to the median value of magnitudes for the POIs discovered by the LSO, adjusted for the wavelength-dependent planetary albedo. (Determining the median required a one-time Monte Carlo experiment for each star.) We also computed the exposure time for spectroscopy for the discovered POI of median brightness, also making an adjustment for the difference in planetary albedo between the wavelength of the LOI to the appropriate wavelength of the spectroscopy. Our input catalog comprised the 116 stars included by Brown (2004) in TPF-C mission studies. Roughly speaking, these are the most favorable main-sequence, non-binary stars for direct detection in reflected starlight. Of these, only 1925 stars were actually observed in the 26119 stellar visits. The reduction of the star list from 116 stars to 19-25 stars occurs in two steps: prior qualification according to pointing restrictions shown in Figure 15, and selection by the scheduling algorithm according to discovery rate. The total possible observing time includes the following sequence: i) Fine-alignment time for the starshade (10h), ii) Initial limiting search observation (LSO) exposure with preferred filter down to the limiting magnitude $\Delta mag_0 = 26$, iii) Time for data downlink, science analysis and decision to followup, rescheduling with target of opportunity (7 days), iv) Fine-Alignment time for the starshade (10h), v) Followup images with NIRCam in the 4 other filters, vi) Time for data downlink, science analysis and decision to followup, rescheduling with target of opportunity (7 days), vii) Fine-alignment time for the starshade (10h), viii) Spectroscopic followup with NIRSpec.

Some 26 of 116 stars qualify for the DRM according to our current estimates of pointing restrictions and time costs. The scheduling algorithm operates on a stack of possible LSOs, prioritized by discovery rate. It picks observations from the top of the stack until a total of 10^7 sec of observing time has been accumulated. For these scheduling purposes, a observation is defined by the Hipparcos number of the star, the preferred filter, the visit number for this star, the probability of a discovery (p), and the discovery rate. For $\eta = 0.3$, for example, the stack for contained 2075 LSOs of 26 stars. When an observation does not make a detection, the observing time cost is just that of the LSO. When a detection occurs, the time cost is the total for the LSO and the characterizing observations. Also, when a detection occurs, all observations of that star are removed from the queue. Because the starshade would be fuel limited to a number of stellar visits of the order of 80, this entire DRM might not fit with the total number of moves. However, because the stars with highest discovery rates are observed first, the truncation of the mission to $\sim$80 visits would not reduce much the expected number of discoveries.

6. CONCLUSION

We studied the science program and design optimization of the New Worlds Probe, an occulting starshade for JWST. Instrument capabilities on-board JWST are well suited for the science goals, and a combination of NIRCam and NIRSpec would enable imaging and spectroscopy of planets and disks. The NWP / JWST combination can image terrestrial planets in the habitable zone of nearby stars, characterize known radial velocity planets in great detail, and measure the brightness and structure of exozodiacal disks interacting with planets. Our Design Reference Mission (DRM) expects a detection and characterization of five Earth-mass planets in the habitable zone of nearby stars, assuming an occurrence rate for such planets of 30%. This DRM includes realistic overheads for starshade operations, and an observing time of 7-9% of JWSTs time over 5 years.[26] Sensitivity calculations show that NWP+JWST can image an Earth-twin at 10 pc in 20 to 80 hours at the 10σ level depending on the filter, and detect water and other molecules (carbon dioxide, methane) in a low-resolution spectrum in $\simeq 10^5$ s between 0.7 and 1.7 μm. These exposure time estimates can be about 10 times shorter for larger terrestrial planets (5 Earth masses). NWP can detect water on a terrestrial planet down to the size of the Earth and therefore characterize the planets habitability, at the 5σ significance level in 73,000 s, and potentially discover oxygen in a Super-Earth, with a 3σ detection of both 0.76 μm and 1.26 μm features in $\simeq 10^6$ s for a 5 Earth-mass planet at 1AU at 10pc. These exposure times can be considerably shortened for more favorable cases for example in 430,000s for the same planet at the inner edge of the habitable zone at 8 pc. It is not entirely clear whether JWST/NIRSpec would fulfill the full promise of the New Worlds Probe with its current filter set. Without the possibility of NIRSpec spectroscopy, a starshade would merely enable broadband images with NIRCam. A pale blue dot image would arguably be an extraordinary discovery, but only a planet spectrum can provide answers to the most exciting questions: What is the composition of the planets atmosphere? Does the planet have liquid water oceans? Is the planet habitable and suitable for life? Can we detect indications of life? One way to substantially reduce the impact of starshade red leak with JWST would be to modify slightly

one of NIRSpecs target acquisition filters with a better out-of-band rejection of 10^5. In addition, the science with a future possible starshade would be significantly improved with a slightly modified bandpass from 0.7 to 1.7 μm.

REFERENCES

[1] C. Marois, B. Macintosh, T. Barman, B. Zuckerman, I. Song, J. Patience, D. Lafrenière, and R. Doyon, "Direct Imaging of Multiple Planets Orbiting the Star HR 8799," *Science* **322**, pp. 1348–, Nov. 2008.

[2] P. Kalas, J. R. Graham, E. Chiang, M. P. Fitzgerald, M. Clampin, E. S. Kite, K. Stapelfeldt, C. Marois, and J. Krist, "Optical Images of an Exosolar Planet 25 Light-Years from Earth," *Science* **322**, pp. 1345–, Nov. 2008.

[3] A.-M. Lagrange, D. Gratadour, G. Chauvin, T. Fusco, D. Ehrenreich, D. Mouillet, G. Rousset, D. Rouan, F. Allard, É. Gendron, J. Charton, L. Mugnier, P. Rabou, J. Montri, and F. Lacombe, "A probable giant planet imaged in the β Pictoris disk. VLT/NaCo deep L'-band imaging," *A&A* **493**, pp. L21–L25, Jan. 2009.

[4] B. A. Macintosh, J. R. Graham, D. W. Palmer, R. Doyon, J. Dunn, D. T. Gavel, J. Larkin, B. Oppenheimer, L. Saddlemyer, A. Sivaramakrishnan, J. K. Wallace, B. Bauman, D. A. Erickson, C. Marois, L. A. Poyneer, and R. Soummer, "The Gemini Planet Imager: from science to design to construction," in *Society of Photo-Optical Instrumentation Engineers (SPIE) Conference Series*, *Society of Photo-Optical Instrumentation Engineers (SPIE) Conference Series* **7015**, July 2008.

[5] J.-L. Beuzit, M. Feldt, K. Dohlen, D. Mouillet, P. Puget, F. Wildi, L. Abe, J. Antichi, A. Baruffolo, P. Baudoz, A. Boccaletti, M. Carbillet, J. Charton, R. Claudi, M. Downing, C. Fabron, P. Feautrier, E. Fedrigo, T. Fusco, J.-L. Gach, R. Gratton, T. Henning, N. Hubin, F. Joos, M. Kasper, M. Langlois, R. Lenzen, C. Moutou, A. Pavlov, C. Petit, J. Pragt, P. Rabou, F. Rigal, R. Roelfsema, G. Rousset, M. Saisse, H.-M. Schmid, E. Stadler, C. Thalmann, M. Turatto, S. Udry, F. Vakili, and R. Waters, "SPHERE: a planet finder instrument for the VLT," in *Society of Photo-Optical Instrumentation Engineers (SPIE) Conference Series*, *Society of Photo-Optical Instrumentation Engineers (SPIE) Conference Series* **7014**, Aug. 2008.

[6] K. W. Hodapp, R. Suzuki, M. Tamura, L. Abe, H. Suto, R. Kandori, J. Morino, T. Nishimura, H. Takami, O. Guyon, S. Jacobson, V. Stahlberger, H. Yamada, R. Shelton, J. Hashimoto, A. Tavrov, J. Nishikawa, N. Ukita, H. Izumiura, M. Hayashi, T. Nakajima, T. Yamada, and T. Usuda, "HiCIAO: the Subaru Telescope's new high-contrast coronographic imager for adaptive optics," in *Society of Photo-Optical Instrumentation Engineers (SPIE) Conference Series*, *Society of Photo-Optical Instrumentation Engineers (SPIE) Conference Series* **7014**, Aug. 2008.

[7] S. Hinkley, B. R. Oppenheimer, D. Brenner, I. R. Parry, A. Sivaramakrishnan, R. Soummer, and D. King, "A new integral field spectrograph for exoplanetary science at Palomar," in *Society of Photo-Optical Instrumentation Engineers (SPIE) Conference Series*, *Society of Photo-Optical Instrumentation Engineers (SPIE) Conference Series* **7015**, July 2008.

[8] M. Mountain, R. van der Marel, R. Soummer, A. Koekemoer, H. Ferguson, M. Postman, D. T. Gavel, O. Guyon, D. Simons, and W. A. Traub, "Comparison of optical observational capabilities for the coming decades: ground versus space," in *astro2010: The Astronomy and Astrophysics Decadal Survey*, *Astronomy* **2010**, pp. 12–+, 2009.

[9] O. Guyon, J. R. P. Angel, D. Backman, R. Belikov, D. Gavel, A. Giveon, T. Greene, J. Kasdin, J. Kasting, M. Levine, M. Marley, M. Meyer, G. Schneider, G. Serabyn, S. Shaklan, M. Shao, M. Tamura, D. Tenerelli, W. Traub, J. Trauger, R. Vanderbei, R. A. Woodruff, N. J. Woolf, and J. Wynn, "Pupil mapping Exoplanet Coronagraphic Observer (PECO)," in *Society of Photo-Optical Instrumentation Engineers (SPIE) Conference Series*, *Society of Photo-Optical Instrumentation Engineers (SPIE) Conference Series* **7010**, Aug. 2008.

[10] W. Cash, P. Oakley, M. Turnbull, T. Glassman, A. Lo, R. Polidan, S. Kilston, and C. Noecker, "The New Worlds Observer: scientific and technical advantages of external occulters," in *Society of Photo-Optical Instrumentation Engineers (SPIE) Conference Series*, *Society of Photo-Optical Instrumentation Engineers (SPIE) Conference Series* **7010**, Aug. 2008.

[11] D. N. Spergel, J. Kasdin, R. Belikov, P. Atcheson, M. Beasley, D. Calzetti, B. Cameron, C. Copi, S. Desch, A. Dressler, D. Ebbets, R. Egerman, A. Fullerton, J. Gallagher, J. Green, O. Guyon, S. Heap, R. Jansen, E. Jenkins, J. Kasting, R. Keski-Kuha, M. Kuchner, R. Lee, D. Lindler, R. Linfield, D. Lisman, R. Lyon, S. Malhotra, G. Mathews, M. McCaughrean, J. Mentzel, M. Mountain, S. Nikzad, R. O'Connell, S. Oey, D. Padgett, B. Parvin, J. Procashka, W. Reeve, I. N. Reid, J. Rhoads, A. Roberge, B. Saif, P. Scowen, S. Seager, O. Seigmund, K. Sembach, S. Shaklan, M. Shull, and R. Soummer, "THEIA: Telescope for Habitable Exoplanets and Interstellar/Intergalactic Astronomy," in *Bulletin of the American Astronomical Society*, *Bulletin of the American Astronomical Society* **41**, pp. 362–+, Jan. 2009.

[12] W. C. Danchi, R. K. Barry, P. R. Lawson, W. A. Traub, and S. Unwin, "The Fourier-Kelvin Stellar Interferometer (FKSI): a review, progress report, and update," in *Society of Photo-Optical Instrumentation Engineers (SPIE) Conference Series*, *Society of Photo-Optical Instrumentation Engineers (SPIE) Conference Series* **7013**, July 2008.

[13] N. J. Kasdin, D. N. Spergel, R. J. Vanderbei, E. Cady, D. Savransky, D. Lisman, S. Shaklan, R. Lee, R. Egerman, G. Matthews, and D. Tenerelli, "A Medium Size Mission for Finding and Characterizing Terrestrial ExoPlanets with an External Occulter and a Conventional Space Telescope," in *Bulletin of the American Astronomical Society*, *Bulletin of the American Astronomical Society* **41**, pp. 287–+, Jan. 2010.

[14] J. P. Gardner, J. C. Mather, M. Clampin, R. Doyon, M. A. Greenhouse, H. B. Hammel, J. B. Hutchings, P. Jakobsen, S. J. Lilly, K. S. Long, J. I. Lunine, M. J. McCaughrean, M. Mountain, J. Nella, G. H. Rieke, M. J. Rieke, H.-W. Rix, E. P. Smith, G. Sonneborn, M. Stiavelli, H. S. Stockman, R. A. Windhorst, and G. S. Wright, "The James Webb Space Telescope," *Space Science Reviews* **123**, pp. 485–606, Apr. 2006.

[15] K. S. Long, "JWST Mission Operations Concept Document (JWST-OPS-002018)," STScI, Baltimore, 2006. Revision B.

[16] W. Cash, E. Schindhelm, J. Arenberg, R. Polidan, S. Kilston, and C. Noecker, "The New Worlds Observer: using occulters to directly observe planets," in *Society of Photo-Optical Instrumentation Engineers (SPIE) Conference Series*, *Society of Photo-Optical Instrumentation Engineers (SPIE) Conference Series* **6265**, July 2006.

[17] W. Cash, D. N. Spergel, R. Soummer, M. Mountain, K. Hartman, R. Polidan, T. Glassman, and A. Lo, "The New Worlds Probe: A starshade with JWST." Request for Information to Astro2010: The Astronomy and Astrophysics Decadal Survey, June 2009.

[18] M. Postman, T. Brown, A. Koekemoer, M. Giavalisco, S. Unwin, W. Traub, D. Calzetti, W. Oegerle, M. Shull, S. Kilston, and H. P. Stahl, "Science with an 8-meter to 16-meter optical/UV space telescope," in *Society of Photo-Optical Instrumentation Engineers (SPIE) Conference Series*, *Society of Photo-Optical Instrumentation Engineers (SPIE) Conference Series* **7010**, Aug. 2008.

[19] M. Postman, "Advanced Technology Large-Aperture Space Telescope (ATLAST): A Technology Roadmap for the Next Decade," *ArXiv e-prints* , Apr. 2009.

[20] J. I. Lunine, D. Fischer, H. Hammel, T. Henning, L. Hillenbrand, J. Kasting, G. Laughlin, B. Macintosh, M. Marley, G. Melnick, D. Monet, C. Noecker, S. Peale, A. Quirrenbach, S. Seager, and J. Winn, "Worlds Beyond: A Strategy for the Detection and Characterization of Exoplanets," *ArXiv e-prints* , Aug. 2008.

[21] R. Soummer, M. Levine, and Exoplanet Forum Direct Optical Imaging Group, *Exoplanet Community Report on Direct Optical Imaging*, ch. 3. http://exep.jpl.nasa.gov/, 2009.

[22] R. Soummer, W. Cash, R. A. Brown, I. Jordan, A. Roberge, T. Glassman, A. Lo, S. Seager, and L. Pueyo, "The New Worlds Probe: A Starshade for JWST," in *Bulletin of the American Astronomical Society*, *Bulletin of the American Astronomical Society* **41**, pp. 290–+, Jan. 2010.

[23] R. A. Brown, "Single-Visit Photometric and Obscurational Completeness," *ApJ* **624**, pp. 1010–1024, May 2005.

[24] D. Savransky, N. J. Kasdin, and E. Cady, "Analyzing the Designs of Planet-Finding Missions," *PASP* **122**, pp. 401–419, Apr. 2010.

[25] D. J. Des Marais, M. O. Harwit, K. W. Jucks, J. F. Kasting, D. N. C. Lin, J. I. Lunine, J. Schneider, S. Seager, W. A. Traub, and N. J. Woolf, "Remote Sensing of Planetary Properties and Biosignatures on Extrasolar Terrestrial Planets," *Astrobiology* **2**, pp. 153–181, June 2002.

[26] R. A. Brown and R. Soummer, "New Completeness Methods for Estimating Exoplanet Discoveries by Direct Detection," *ApJ* **715**, pp. 122–131, May 2010.